Determination of Surface Area and Porosity of Small, Nanometer-Thick Films by Quartz Crystal Microbalance Measurement of Gas Adsorption†

Yoshitaka Aoki,‡ Mineo Hashizume,§ Shinya Onoue,⊥ and Toyoki Kunitake*

Topochemical Design Laboratory, Frontier Research System, RIKEN, 2-1 Hirosawa, Wako, Saitama 351-0198, Japan

Received: March 2, 2008; Revised Manuscript Received: April 20, 2008

The Brunauer−Emmett−Teller (BET) surface area of 15 nm-thick films made of TiO_2/polyelectrolyte bilayer was determined by quartz crystal microbalance (QCM) measurement of N_2 and Ar adsorption isotherms at 77 K. The measurements were carried out using a home-built vacuum chamber that includes built-in 9 MHz QCM and cryostat units. As little as 1 ng of the adsorbed gas could be detected, and the BET surface area of a flat Au film (ca. 0.5 cm^2) on an oscillator was determined within an experimental error of ±5%. The titania/polymer composite film gives N_2 and Ar adsorption isotherms consisting of a less-pronounced type-I curve and a break at around $p/p_0 = 0.7$. This behavior is ascribed to the presence of irregular micropores and 6 nm ϕ-mesopores in the composite film. An analysis of the isotherms shows that the porosity of the composite film is about 12%, which is much smaller than that of bulk titania gel powder. The greater density appears to be related to the reported superior properties (robustness and resistance to electrical breakdown) of the organic/inorganic multilayer film. We conclude that the QCM-based, high-precision measurement of gas adsorption is a powerful tool for investigation of the detailed morphology of nanometer-thick films.

Introduction

Nanometer-thick films with designed compositions and microstructures occupy a central position in the nanomaterials research. In particular, self-supporting ultrathin films of metal oxide/polymer composite have attracted considerable attention because of their unique geometrical and mechanical properties,[1–4] as well as their potential applications for mass separation, filter, sensors, etc.[5–9] Recently, Kunitake et al. fabricated self-supporting films of metal oxide and/or polymer composites with thicknesses of few tens of nanometers on the basis of the sol−gel process[10–13] and reported that some of these films exhibited superior mechanical properties, bearing the weight 10^4 times greater than their own.[10,13] These superior properties must be strongly related to the structural uniformity with small density of structural defects (voids and pores) in the microscopic and mesoscopic scales. Therefore, it is important to make precise evaluation of such structural defects. The gas adsorption isotherm technique is an effective method to estimate the size and volume of pores in various materials. Unfortunately, the conventional technique of gas adsorption isotherm is based on a volumetric method and is difficult to apply to small samples with surface areas of less than 1 m^2. It is strongly desired in nanomaterials research to develop a way to characterize the morphology of nanometer-thick films. Quartz crystal microbalance (QCM)[14–20] and surface acoustic wave devices[21,22] have been examined for measurement of the surface area of thin films by the gas adsorption technique, since these devices are able to detect a nanogram mass increase. Krim has extensively studied gas adsorption on fractal rough surfaces of metal thin films (∼100 nm thick) by QCM[14–18] and, in particular, measured adsorption isotherms of N_2, Ar, Kr, Xe, and CH_4 at temperatures below their triple points by constructing a vacuum cell system equipped with cryostat.[18] Such a system may be equally suitable for quantitative analysis of the amounts of voids in nanofilms. In this article, we describe successful measurement of N_2 and Ar adsorption isotherms of a nanometer-thick metal oxide/polymer composite film by directly detecting adsorbed masses with a 9 MHz quartz crystal microbalance. The Brunauer−Emmett−Teller (BET) surface area and micropore volume of the nanofilm could be precisely determined. These results indicate that detailed examination of micromorphology of ultrathin films is now possible. Combination of such direct measurement with TEM and AFM observations will be a powerful tool to characterize morphologies of ultrathin films.

Experimental Methods

Film Fabrication. The quartz resonator employed in this study is of the "AT cut type" with 8.6 mm ϕ and 0.2 mm thickness, and the fundamental frequency is 9 MHz. Each side of the quartz crystal plate was covered by a deposition of gold film electrodes with an adsorption-active area of $A = 0.156$ cm^2 and a thickness of ∼100 nm. The surface of the Au film electrode was cleaned by a piranha solution (H_2SO_4/H_2O_2 = 7/3), rinsed in Milli-Q water, and dried by nitrogen blow, and this Au film was used as a reference sample of gas adsorption experiments.

The ultrathin film made of a TiO_2/polyelectrolyte bilayer was prepared on the Au electrode by the method described elsewhere.[23] The surface of the Au electrode was modified by self-assembled monolayer of mercaptoethansulfonate ($HSC_2H_4SO_3H$) so as to form the negatively charged surface.[23] The alternative multilayer of poly(diallyldimethylammonium chloride) (PDDA, MW

† Part of the "Janos H. Fendler Memorial Issue".

* Corresponding author. Address: NanoMembrane Technologies, Inc., Wako-RIKEN IP 406, 2-3-13 minami, Wako, 351-0104, Japan. Phone: +81-48-299-3226. Fax: +81-48-299-3227. E-mail: kunitake@ruby.ocn.ne.jp.

§ Current address: Graduate School of Materials Science, Nara Institute of Science and Technology (NAIST), 8916-5 Takayama, Ikoma, Nara, 630-0192 Japan.

‡ Current address: Graduate School of Engineering, Hokkaido University, Kita-13 Nishi-8, Kita-ku, Sapporo, 060-8628, Japan.

⊥ Current address: Kyoritsu Chemical & Co., Ltd., 4-18-2 Shiomi, Kisarazu, Chiba, 292-0834 Japan.

10.1021/jp801919h CCC: $40.75
Published on Web 07/01/2008

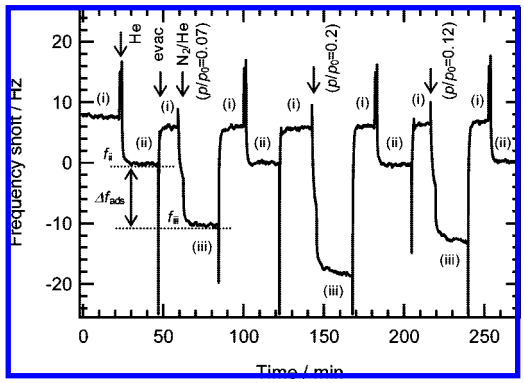

Figure 1. Response transient of frequency shifts of QCM due to N_2 adsorption on Au film electrode at 77 K. Step i: evacuating; step ii, pure He atmosphere at a total pressure of 90 kPa; and step iii, N_2/He mixed gas atmosphere at adjusted N_2 partial pressures (p/p_0) (total pressure of 90 kPa).

240 000, Polyscience) and poly(acrylic acid) (PAA, MW 18 000, Aldrich) was prepared on the modified QCM by electrostatic alternate assembly.[24] These polymer layers function as an adsorbent for $Ti(O^nBu)_4$ because of the electrostatic interaction between partially hydrolyzed $Ti(O^nBu)_4$ and positive charge of PDDA and the coordination of carboxyl groups of PAA to Ti atom.[23,25] The multilayer of $(PDDA/PAA)_3$ with the outermost PAA layer was assembled by alternate immersion (three cycles) of a modified QCM into a 1 mg mL^{-1} aqueous solution of PDDA and into a 1 mg mL^{-1} aqueous solution of PAA at room temperature for 1 min, followed by rinsing in Milli-Q water for 1 min and drying by nitrogen blow. Then, the TiO_x−gel layer was built up on the precursor film by immersion in a 100 mM solution of $Ti(O^nBu)_4$ in 1:1 (v/v) toluene/ethanol for 3 min, rinsed in ethanol for 1 min, hydrolyzed in Milli-Q water for 1 min, and dried by nitrogen blow. The details of the surface sol−gel process were described elsewhere.[25,26]

Apparatus. A homemade gas flow chamber system equipped with a rotary pump, computer-adjusted mass flow controller, and cryostat was constructed for QCM measurement of the N_2 and Ar adsorption isotherm at 77 K. The sample cell made of a stainless steel tube with dimensions of ϕ 25 mm and L 350 mm is rubber-sealed and contains the quartz crystal resonator. To monitor temperature near the resonator, a Pt resistance thermometer (Pt100) was placed only 2 mm apart from the resonator. The sample cell was placed inside a liquid nitrogen bath and was kept at 77 K. Ultrapure grade gases (>99.9999%) were used for all measurements. A measuring gas was introduced into the cell through the stainless tube after removing humidity and molecular oxygen by passing it through the gas-purifier column (GL science). The partial pressure of adsorbate vapor (N_2 and Ar) was adjusted by changing their flow rates and further dilution with a He stream. The flow rate was controlled by the computer-adjusted mass flow controller (Koflok 3440). The evacuation of the cell was performed by using a rotary vacuum pump (Edward RV12). The total pressure in the sample cell was measured by a capacitance manometer gauge (Pfeifer CMR271). A quartz crystal microbalance device manufactured by USI System (Fukuoka Japan) was used. A quartz resonator in the sample cell was electrically connected to the oscillator circuitry through the Cu wire. The signal from the oscillator circuitry was monitored by a frequency analyzer (HP 5111) and stored on a PC.

QCM Measurement. The mass of adsorbed gases was determined as follows. The sample resonator was mounted in the cell and heated at 150 °C for 2 h under evacuation to degas the sample before the adsorption experiment. First, the sample cell was kept at 77 K and evacuated to less than 0.01 Pa (step i). Then, the evacuation was stopped, and pure He gas was introduced into the chamber until the pressure reached 9×10^4 Pa (step ii) at 77 K. Since adsorption of He gas onto the solid surface is known not to occur at 77 K, the equilibrium frequency in step ii can be defined as a blank frequency, f_{ii}, of the adsorption at 77 K and 9.0×10^4 Pa. The cell was evacuated again to less than 0.1 Pa (step i) and finally, a mixture of He and adsorbent (N_2 or Ar) with an appropriate molar ratio was admitted at a total pressure, P_{tot}, of 9.0×10^4 Pa (step iii), and the new frequency after equilibrium of adsorption is obtained as f_{iii}. The gas adsorption, Δf_{ads}, is defined as

$$\Delta f_{ads} = f_{iii} - f_{ii} \quad (1)$$

The mass of adsorbed gas is determined from Δf_{ads} by the Sauerbrey equation,

$$\Delta f_{ads} = \frac{-2f_0^2 \Delta m}{A\sqrt{\rho_q \mu_q}} \quad (2)$$

where f_0 is the fundamental frequency of the crystal, Δm is the mass of the adsorbed gas; $\mu_q = 2.95 \times 10^{11}$ g cm^{-1} and $\rho_q = 2.65$ g cm^{-3} are the shear modulus and the density of quartz, respectively; and A is the area of geometrically flat surface of an electrode on a major face of the crystal.[27] The resonator used here gives $\Delta m = 0.851 \times \Delta f_{ads}$ (ng). These measuring procedures were repeated many times in the sequence of I → ii → I → iii → •••• with different partial pressures of the adsorbent, p/p_0, in step iii to give the gas adsorption isotherm.

Results and Discussion

As a first step, gas adsorption on a Au electrode coated QCM resonator was examined to ascertain the reliability of our system. Figure 1 shows the response transient of frequency changes of QCM due to gas adsorption at 77 K. The details of the experimental procedure are described in the Experimental Section. The sample cell is evacuated at 10^{-2} Pa for more than 20 min as temperature is maintained at 77 K (step i), and then a pure He gas with a total pressure of 9.0×10^4 Pa is supplied to the evacuated cell (step ii). With the introduction of He gas, the oscillator frequency is quickly lowered by ~5 Hz and reaches equilibrium within a few seconds (f_{ii}). Since adsorption of He gas should be negligible at this temperature, this frequency shift is attributed to the effect of pressure change,[19] and therefore, the f_{ii} value can be defined as the pressure-correction frequency at 77 K and 9.0×10^4 Pa. When N_2/He mixed gas (N_2 partial pressure, p/p_0 of 0.07) is supplied at a total pressure of 9.0×10^4 Pa (step iii) after reevacuating pure He gas, the frequency quickly decreases additionally due to N_2 adsorption. It reaches equilibrium within a few minutes (f_{iii}). The neat frequency shift due to the adsorption of N_2 and other gases can be estimated from $f_{iii} - f_{ii}$. The pressure-correction frequency (f_{ii}) is constant within ±0.1 Hz during a given measurement that lasts for several hours. In addition, the fluctuation of frequency in step iii is less than ±1.3 Hz at any p/p_0. Therefore, the experimental error is calculated to be within ±1.4 Hz, corresponding to an accuracy of mass detection of ±1.2 ng. With our QCM setup, monolayer coverage over the flat active electrode areas (0.156×2 cm^2) is calculated to correspond to a frequency shift of 10.8 Hz by employing the density of 2-dimensional liquid nitrogen (34.5 ng cm^{-2}).[16] On the basis of these results, it is estimated that our method can determine the BET surface area within a error of less than 10%.

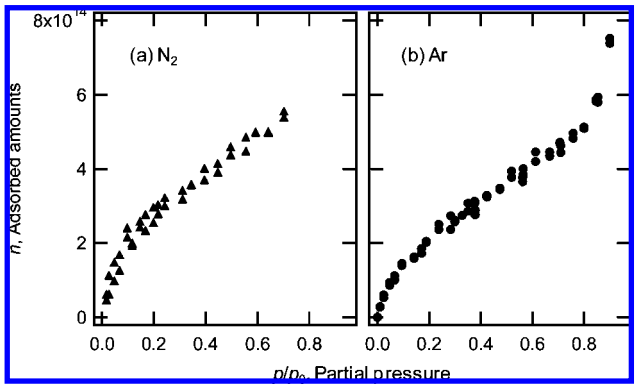

Figure 2. Adsorption isotherms of N_2 (a) and Ar (b) on a Au film electrode at 77 K.

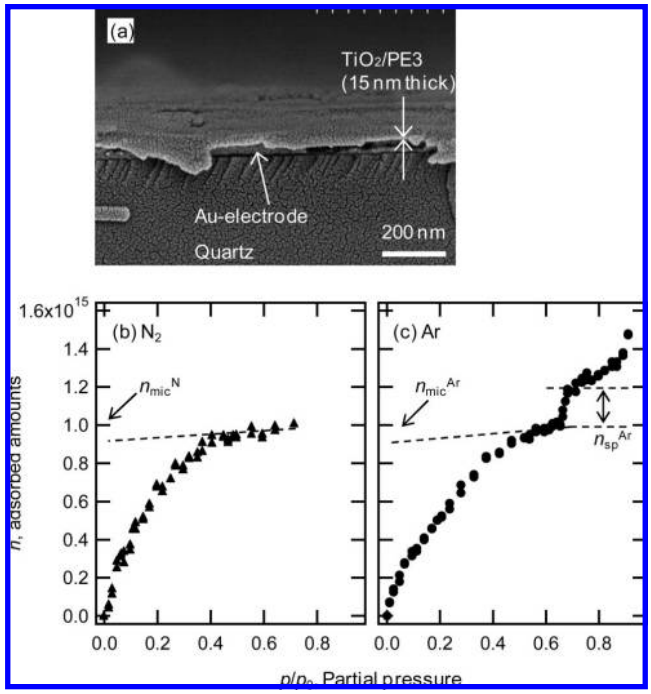

Figure 3. (a) Cross section SEM image of ultrathin TiO_2/PE3 composite film prepared on Au electrode of resonator. Adsorption isotherms of N_2 (b) and Ar (c) on the TiO_2/PE3 composite film at 77 K.

Adsorption isotherms of N_2 and Ar on bare Au electrode are obtained by plotting the number of the adsorbed N_2 molecules (n) as a function of p/p_0 (Figure 2). Precise QCM measurements were difficult under high N_2 concentrations in the rage of $p/p_0 > 0.7$, since the temperature in the sample cell could not reach 77 K. The fundamental frequency is highly sensitive to minor temperature changes.[19] In contrast, the cell temperature can be maintained stably at 77 K at all p/p_0 ranges in the case of Ar. Such contrasting behavior may arise from the relatively large heat capacitance of N_2 as compared to Ar.[28] At $p/p_0 < 0.7$, the two isotherms have similar curves. The adsorbed gases are rapidly equilibrated at $p/p_0 < 0.05$ and linearly increase in proportion to p/p_0 in the range of $0.05 < p/p_0 < 0.7$. The amount of adsorbed Ar exponentially increases at the higher pressure region ($p/p_0 > 0.70$), and the isotherms exhibit upward deviation from the linearity. These features of Ar and N_2 isotherms are identical to those of the multilayer adsorption on flat surfaces (type II curve of IUPAC classification[29]). Accordingly, the adsorption isotherm is analyzed by the classical Brunauer−Emmett−Teller, BET, method which is generally used to determine the monolayer coverage (n_m) that is the number of molecules required for covering the surface in a monolayer. In the BET model, the adsorption of molecules on the surface can be expressed by the following equation:[30]

$$\frac{p/p_0}{n(1-p/p_0)} = \frac{1}{n_m c} + \frac{c-1}{n_m c}(p/p_0) \qquad (3)$$

Here, n is the number of adsorbed molecules, and c is a constant. This model is applicable to the adsorption of gases up to a few monolayers; therefore, n_m is calculated from the isotherm data in the low p/p_0 region ($p/p_0 < 0.2$ by the usual method).[30] The BET surface area, S_{BET}, was calculated from the n_m and molecular areas of adsorbate gases at 77 K. Conventionally, molecular areas of N_2 (a^N) and Ar (a^{Ar}) are calculated from the density of the liquid at the temperature, as 0.162 nm^2 and 0.138 nm^2, respectively.[29,30] On the basis of these data, the BET surface area of the Au film electrode was calculated to be 0.54 cm^2 from the N_2 isotherm (S^N_{BET}) and to be 0.37 cm^2 from Ar isotherm (S^{Ar}_{BET}) (Table 1). S^{Ar}_{BET} is clearly smaller than S^N_{BET}. Rouquerol et al. reported that the S^{Ar}_{BET} of nonporous and porous silica powders is more precisely determined by using an a^{Ar} of 0.182 nm^2 rather than 0.138 nm.[230] By using this new a^{Ar} value, the S^{Ar}_{BET} of the Au film is calculated to be 0.50 cm^2, consistent with that of the S^N_{BET}. The surface roughness factor (r_{sa}), the ratio of geometrical surface area to flat surface area, of the Au electrode is calculated to be 1.7. This r_{sa} value is close to that of a 100-nm-thick Au film, as determined by STM (2.0).[19,31] It is clear that the current QCM method is reliably employed to measure a surface area as small as 0.1 cm^2.

TABLE 1: Analysis of N_2 and Ar Adsorption on a Au Film Electrode and on a TiO_2/PAA Composite Film

	N_2	Ar
Au film: 100 nm thick		
BET monolayer capacity, n_m		
BET surface area, S_{BET} (cm^2)	0.54	0.50
TiO_x−Gel/Polymer Thin Film: 15 nm Thick, 792 ng		
BET monolayer capacity, n_m	6.8×10^{14}	5.7×10^{14}
BET surface area, S_{BET} (cm^2)	1.1	1.0
(m^2 g^{-1})	140	130
micropore capacity, n_{mic}	9.2×10^{14}	9.3×10^{14}
micropore volume, V_{mic}		
(cm^3)	5.3×10^{-8}	4.7×10^{-8}
(cm^3 g^{-1})	0.067	0.059
(vol %)	11	10
6 nmϕ-pore capacity, n_{sp}		1.9×10^{14}
6 nmϕ-pore volume, V_{sp}		
(cm^3)		9.6×10^{-9}
(cm^3 g^{-1})		0.012
(vol %)		2.0

Subsequently, gas adsorption isotherms of an ultrathin metal oxide/polymer composite film were examined in the same way. Ultrathin composite films of TiO_2 on the alternate layer of poly(diallyldimethylammonium) (PDDA) and poly(acrylic acid) (PAA), TiO_2/[PAA/PDDA]$_3$, was prepared by the method described elsewhere.[23] Hereafter, the polyelectrolyte multilayer, [PAA/PDDA]$_3$, is denoted as PE3, and the TiO_2/[PAA/PDDA]$_3$ is represented as TiO_2/PE3. As shown in the SEM image of Figure 3a, the composite film is uniformly formed with a thickness of 15 nm, and it fully covers the surface of the Au electrode. The weight of the PE3 layer and the TiO_2 layer were 209 and 583 ng, respectively, from the frequency shift of QCM after deposition of each layer.

N_2 and Ar adsorption isotherms of the TiO_2/PE3 composite film are shown in Figure 3b and c, respectively. The shapes of

these isotherms are clearly different from those of the Au film electrode. In the case of N_2 adsorption, the amount of gas adsorption logarithmically increases at $p/p_0 < 0.4$ and becomes saturated in the range of $0.4 < p/p_0 < 0.7$. The Ar adsorption isotherm of Figure 3c exhibits a similar behavior at $p/p_0 < 0.7$, with a gradual increase in Ar adsorption at $p/p_0 < 0.5$ and saturation in the range of $0.5 < p/p_0 < 0.7$. However, it exhibits a small "gap" at $p/p_0 = 0.67$ by a rapid increase probably due to the capillary condensation of liquid Ar in a mesopore, as discussed later.

A Type I curve is characteristic of the adsorption on well-defined microporous materials, such as zeolite, porous carbon, and a molecular cage crystal. It is composed of a rapid rise in adsorption in the very low p/p_0 region (typically, <0.05) and saturation in the higher p/p_0 range.[29,30] On the other hand, mesoporous materials show the type IV curve that is similar to the type II curve in the initial region but levels off at a relatively high pressure region.[30] The two adsorption isotherms of the composite film are close to a type I curve rather than a type IV curve, and the Ar isotherm shows leveling off, as is the case with a type IV curve. It is reported that hydrous metal oxide gels contain a large amount of pores ranging from microscopic to mesoscopic scales to show a less-pronounced type I curve, consisting of a logarithmic curve at low pressures and saturation at high pressures.[30,32] From this comparison, the observed feature of isotherm curves of the composite film may be attributed to the presence of irregular pores of different sizes.

The BET surface area of the TiO_2/PE3 composite film was estimated from the isotherm data at $p/p_0 < 0.2$ (Table 1). The S^{N}_{BET} value of 1.1 cm^2 as calculated with an a^N of 0.162 nm^2 is in satisfactory agreement with a S^{Ar}_{BET} of 1.0 cm^2 as calculated with an a^{Ar} of 0.182 nm^2. The presence of plateaus observed at $0.4 < p/p_0 < 0.7$ for N_2 and at $0.5 < /p_0 < 0.7$ for Ar can be attributed to the micropore filling. Adsorption capacity of micropores (n_{mic}) in the film was determined from the adsorption in the saturation region (plateau) by the "Point-B" method (Figure 3b),[30] which determines the monolayer capacity from the point defined as the beginning of the middle linear region.[30,33] Thus, the total micropore volume (V_{mic}) was calculated using the n_{mic} value and liquid densities of N_2 and Ar at 77 K[30,34,35] (Table 1). Values of n_{mic} and V_{mic} agree between the N_2 and Ar isotherms (n^{N}_{mic} is 9.2×10^{14}, n^{Ar}_{mic} is 9.3×10^{14}, V^{N}_{mic} is 5.3×10^{-8} cm^3; and V^{Ar}_{mic} is 4.7×10^{-8} cm^3). Furthermore, values of n_{mic} are consistent with the value of the monolayer capacity (n_m) determined by the BET method. The volume of the TiO_2/PE3 composite film is estimated to be 4.7×10^{-7} cm^3 from the film thickness (15 nm) and the active electrode area of the resonator (0.156×2 cm^2). Accordingly, the volume fraction of micropores in the composite film is calculated as 10%.

The leveling off of adsorption at $p/p_0 = 0.67$ is clearly observed in the Ar curve. This suggests the presence of the capillary condensation of Ar in a cylindrical hollow structure. It appears that pores with a specific size open on the surface of the composite nanofilm. Such behavior is not observed with the N_2 curve. The onset of pore-filling by N_2 gas should occur at pressures higher than that for Ar gas, according to the density functional theory.[36] Therefore, the capillary condensation by N_2 adsorption within the pore must occur at the p/p_0 range higher than the measurable upper limit (0.7) in our setup.

Jaroniec reported that the pore radius, $r_c(p/p_0)$, can be determined from the Ar adsorption isotherm at 77 K by using the modified Kelvin equation,

$$r_c(p/p_0) = -\gamma v/RT \log(0.8259\, p/p_0) + 0.343 + t(p/p_0) \quad (4)$$

where γ and v are viscosity and molar volume of Ar liquid at 77 K, respectively; $t(p/p_0)$ is the thickness of the Ar 2D liquid at p/p_0; and the other numbers are empirical constants.[35] The diameter of the pore related to capillary condensation in a film ($2r_c(0.67)$) is calculated as 6 nm from the onset pressure ($p/p_0 = 0.67$), properties of Ar liquid[34,35] and $t(p/p_0)$ of commercial silica gel.[35] The adsorption capacity of the 6 nm ϕ-pore (n^{Ar}_{sp}) is estimated to be 1.9×10^{14} from the gap width at the onset point (Figure 3b), and the volume of the 6 nm ϕ-pore (V_{sp}) is calculated to be 9.6×10^{-9} cm^3. This value corresponds to the volume fraction of 2.0% of the whole volume of the TiO_2/PE3 film.

On the basis of these results, the porosity of a composite film is estimated to be approximately 12 vol %, and the total specific pore volume, including irregular micropores and 6 nm ϕ-pore, is calculated to be 0.07−0.08 cm^3 g^{-1} from the pore volume and the film weight of Table 1. This value is quite small when compared with that of the bulk TiO_x gel powders prepared by the precipitation method (0.7 cm^3 g^{-1}).[37] Therefore, the ultrathin composite film contains many fewer micropores, microcracks, and pinholes as compared with the corresponding bulk materials. The polyelectrolyte underlayer in our composite film contains large amounts of free carboxyl and ammonium functional groups, creating dense surface adsorption sites for metal alkoxide molecules. Accordingly, the metal alkoxide will be tightly and uniformly adsorbed on the polymer layer so as to form a dense composite film. Formation of such dense films may be related to superior mechanical and electrical properties. In fact, we have previously observed that metal oxide dielectric films prepared by layer-by-layer deposition reveal dielectric breakdown at an electric field much higher than that of the identical film prepared by the conventional, macroscopic sol−gel process.[38]

The size of 6 nm observed for the specific pore (at the volume fraction of only 2.0%) is much larger than that of the mean pore diameter of layer-by-layer assembled polyelectrolyte films (0.5−2 nm), as determined by NMR spectroscopy.[39] In fact, this size is too large relative to the film thickness of 15 nm. Therefore, such a large pore may exist only on the surface of the uppermost titania layer (not in the film interior). This supposition is consistent with the overall small porosity of the composite film. It is possible that rapid hydrolysis of certain fractions of the metal alkoxide by the residual water on the hydrophilic polyelectrolytes layer leads to formation of such large pores.

Conclusions

It is demonstrated that the mass of the adsorbed gas is directly determined at 77 K by using the 9 MHz QCM system equipped with a vacuum gas chamber and cryostat. This technique enables reliable measurement of the gas adsorption isotherm of small, nanometer-thick films: surface areas on the order of 0.1 cm^2 and a pore volume on the order of 10^{-9} cm^3. According to the current results, the metal oxide film prepared on a polyelectrolyte layer is much more uniform and contains lesser concentrations of voids and cracks, as compared with a bulk metal oxide gel powder. It is noteworthy that the QCM isotherm technique is sensitive enough to detect a pore of a few vol % in an ultrathin nanofilm.

The pore-size distribution in the porous nanomaterials will be determined by combining our QCM method and the BJH or DI algorithms.[30] Recently, nanometer-thick films of mesoporous

silica and polymer have attracted much attention as low-κ interconnect materials of ultralarge-scale integrated circuits.[40] The structural analysis of these porous nanofilms by the gas adsorption technique should be very useful. There is a strong demand to investigate the gas-accessible surface in inter- and intraspaces of carbon nanotube bundles to clarify the mechanism of their H_2 sorption properties.[33,41,42] Since our QCM method is applicable to the measurement of surface area and inner pores of most solid nanomaterials, it should be a powerful tool to elucidate the internal structure of nanoarchitectures.

References and Notes

(1) Stroock, A.; Kane, R. S.; Weck, M.; Metallo, S. J.; Whitesides, G. M. *Langmuir* **2003**, *19*, 2466.
(2) Vendamme, R.; Ohzono, T.; Nakao, A.; Shimomura, M.; Kunitake, T. *Langmuir* **2007**, *23*, 2792.
(3) Burghard, Z.; Tucic, A.; Jeurgens, L. P. H.; Hoffman, R. C.; Bill, J.; Aldinger, F. *Adv. Mater.* **2007**, *19*, 970.
(4) Markutsya, S.; Jiang, C.; Pikus, Y.; Tsukruk, V. V. *Adv. Funct. Mater.* **2005**, *15*, 771.
(5) Jiang, C.; Markutsya, S.; Pikus, Y.; Tsukruk, V. V. *Nat. Mater.* **2004**, *3*, 721.
(6) O'Connel, P. A.; McKenna, G. B. *Science* **2005**, *307*, 1760.
(7) Striemer, C. C.; Gaborski, T. R.; McGrath, J. L.; Fauchart, P. M. *Nature* **2007**, *445*, 749.
(8) Huck, W. T.; Stroock, A. D.; Whitesides, G. M. *Angew. Chem. Int. Ed.* **2000**, *39*, 1058.
(9) LeMieux, M. C.; McConney, M. E.; Lin, Y.-H.; Singamaneni, S.; Jiang, H.; Bunning, T. J.; Tsukruk, V. V. *Nano Lett.* **2006**, *6*, 730.
(10) Richard, V.; Onoue, S.; Nakao, A.; Kunitake, T. *Nat. Mater.* **2006**, *5*, 494.
(11) Hashizume, M.; Kunitake, T. *Soft Matter* **2006**, *2*, 135.
(12) Hashizume, M.; Kunitake, T. *Langmuir* **2003**, *19*, 10172.
(13) Watanabe, H.; Vendamme, R.; Kunitake, T. *Bull. Chem. Soc. Jpn.* **2007**, *80*, 433.
(14) Panella, V.; Krim, J. *Phys. Rev. E* **1994**, *49*, 4179.
(15) Pfeifer, P.; Wu, Y. J.; Cole, M. W.; Krim, J. *Phys. Rev. Lett.* **1989**, *62*, 1997.
(16) Wang, C. L.; Krim, J.; Toney, M. F. *J. Vac. Sci. Technol., A* **1989**, *7*, 2481.
(17) Chiarello, R.; Penella, V.; Krim, J.; Thompson, C. *Phys. Rev. Lett.* **1991**, *67*, 3408.
(18) Krim, J.; Watts, E. T. *Proc. 3rd Int. Conf. Fundam. Adsorpt.*, 1989, 445.
(19) Tsionsky, V.; Gileadi, E. *Langmuir* **1994**, *10*, 2830.
(20) Yan, Y.; Bein, T. *J. Phys. Chem.* **1992**, *96*, 9387.
(21) Ricco, A. J.; Frey, G. C.; Martin, S. J. *Langmuir* **1989**, *5*, 273.
(22) Taylor, D. J.; Fleig, P. F.; Hietala, S. L. *Thin Solid Films* **1998**, *332*, 257.
(23) He, J.; Fujikawa, S.; Kunitake, T.; Nakao, A. *Chem. Mater.* **2003**, *17*, 3308.
(24) Decher, G. *Science* **1997**, *277*, 1232.
(25) Ichinose, I.; Kawakami, T.; Kunitake, T. *Adv. Mater.* **1998**, *10*, 535.
(26) Ichinose, I.; Senzu, H.; Kunitake, T. *Chem. Mater.* **1997**, *9*, 1296.
(27) Sauerbrey, G. *Z. Phys.* **1959**, *155*, 206.
(28) *Thermophysical Properties of Matter*; The TPRC Data series,*Vol. 4*; Plenum Press:New York, 1970.
(29) Sing, K. S. W.; Everett, D. H.; Haul, R. A. W.; Moscou, L.; Pierotti, R. A.; Rouquerol, J.; Siemieniewska, T. *Pure Appl. Chem.* **1985**, *57*, 603.
(30) Rouquerol, F.; Rouquerol, J.; Sing, K. *Adsorption by Powders & Porous Solids*; Academic Press: London, 1999.
(31) Denley, D. R. *J. Vac. Sci. Technol., A* **1990**, *8*, 603.
(32) Uekawa, N.; Kaneko, K. *J. Phys. Chem. B* **1998**, *102*, 8719.
(33) Krungleviciute, V.; Heroux, L.; Talapatra, S.; Migone, A. D. *Nano Lett.* **2004**, *4*, 1133.
(34) Kruck, M.; Jaroniec, M. *Chem. Mater.* **2000**, *12*, 222.
(35) Kruck, M.; Jaroniec, M. *J. Phys. Chem. B* **2002**, *106*, 4732.
(36) Ravikovitch, P. I.; Wei, D.; Chueh, W. T.; Haller, G. L.; Neimark, A. V. *J. Phys. Chem. B* **1997**, *101*, 3671.
(37) Ragai, J.; Sing, K. S. W. *J. Colloid Interface Sci.* **1984**, *101*, 369.
(38) Aoki, Y.; Kunitake, T.; Nakao, A. *Chem. Mater.* **2005**, *17*, 450.
(39) Chavez, F. V.; Schonhoff, M. *J. Chem. Phys.* **2007**, *126*, 104705.
(40) Lee, H.-J.; Soles, C. L.; Liu, D.-W.; Bauer, B. J.; Wu, W.-L. *J. Polym. Sci. B: Polym. Phys.* **2002**, *40*, 2170.
(41) Shi, W.; Johnson, J. K. *Phys. Rev. Lett.* **2003**, *91*, 015504.
(42) Migone, A. D.; Talapatra, S. In *Encyclopedia of Nanoscience and Nanotechnology*; Nalwa, H. S. Eds.;American Scientific Publisher: Stevenson Ranch, CA, 2004; *Vol. 4*.

JP801919H